

Vertical coupling and transport in high-latitude ionosphere

Dimitry Pokhotelov

Institute for Solar-Terrestrial Physics
German Aerospace Centre (DLR), Neustrelitz

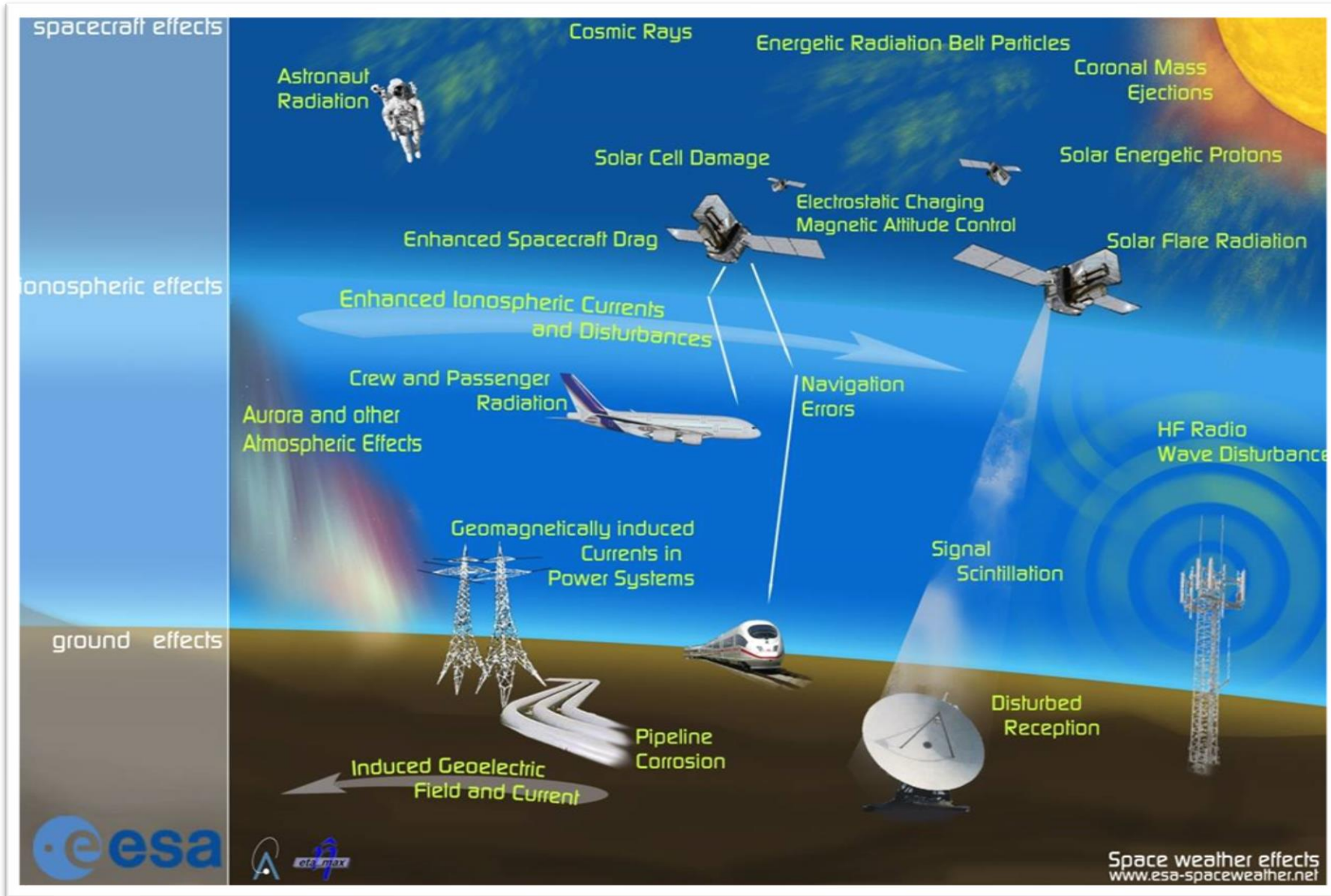
16th IMAGE Meeting
Helsinki, 6-Oct-2022



Knowledge for Tomorrow

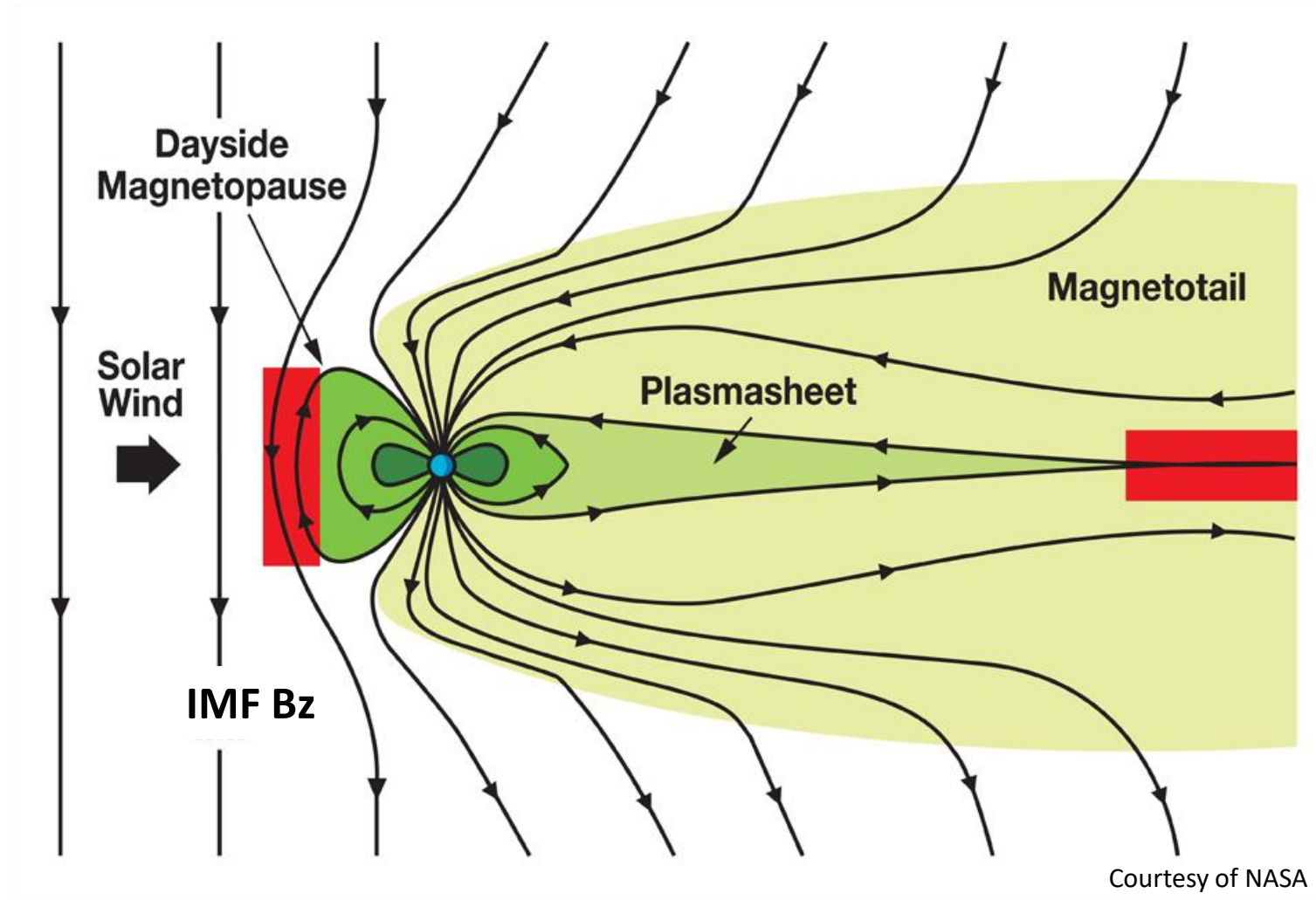


Intro: Space weather



Earth's Magnetosphere

- Magnetosphere is the region of space where the Earth's own magnetic field dominates.
- Under southward IMF conditions, the merging of magnetic field lines is possible at the nose of magnetosphere (dayside reconnection).
- Closed magnetic field lines have both ends linked to the Earth; open field lines have one end linked to the solar wind.

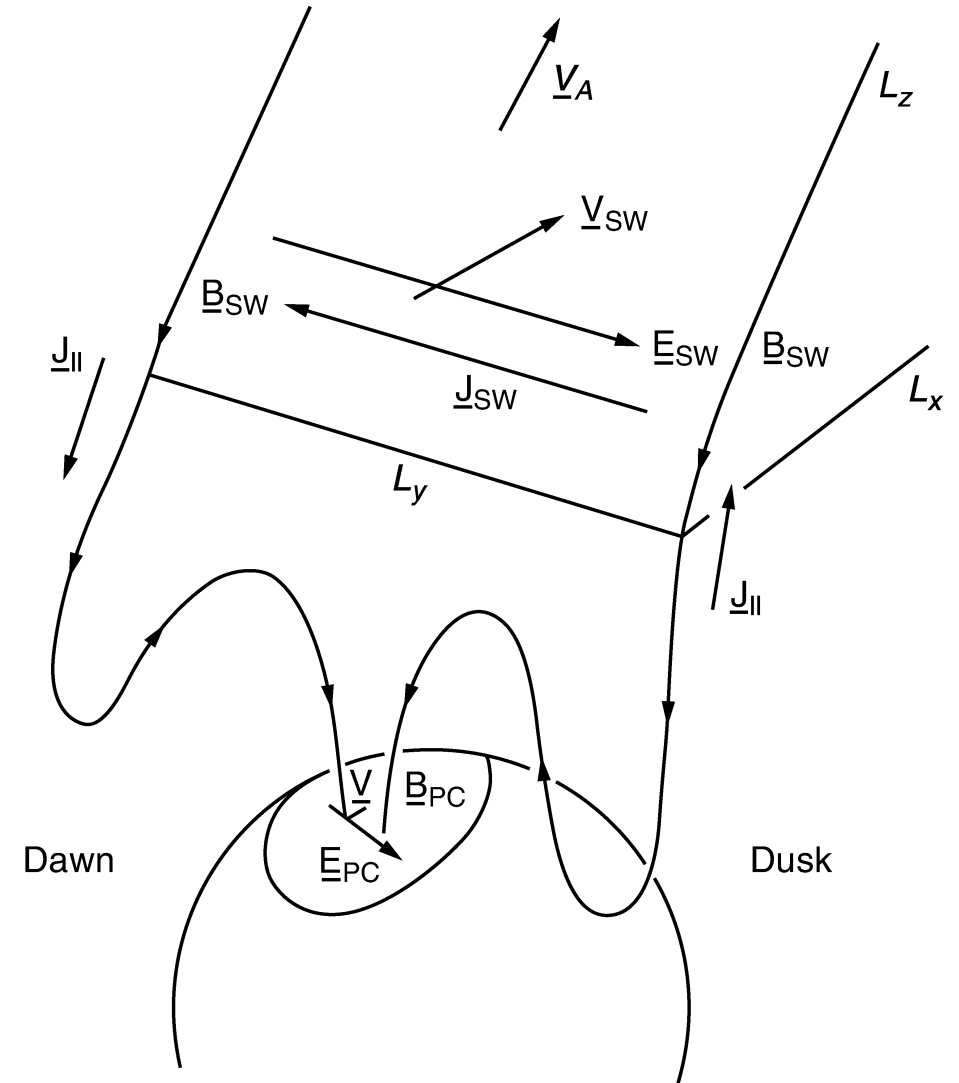


Coupling under southward IMF

Solar wind electric field (frozen-in plasma)

$$\mathbf{E}_{\text{SW}} = -\mathbf{V}_{\text{SW}} \times \mathbf{B}_{\text{SW}}$$

Under a southward IMF, a dawn-to-dusk solar wind electric field \mathbf{E}_{SW} maps to the polar cap ionosphere.



Satellite navigation systems

GPS system

~ 30 navigational GPS spacecraft

55° inclination orbits

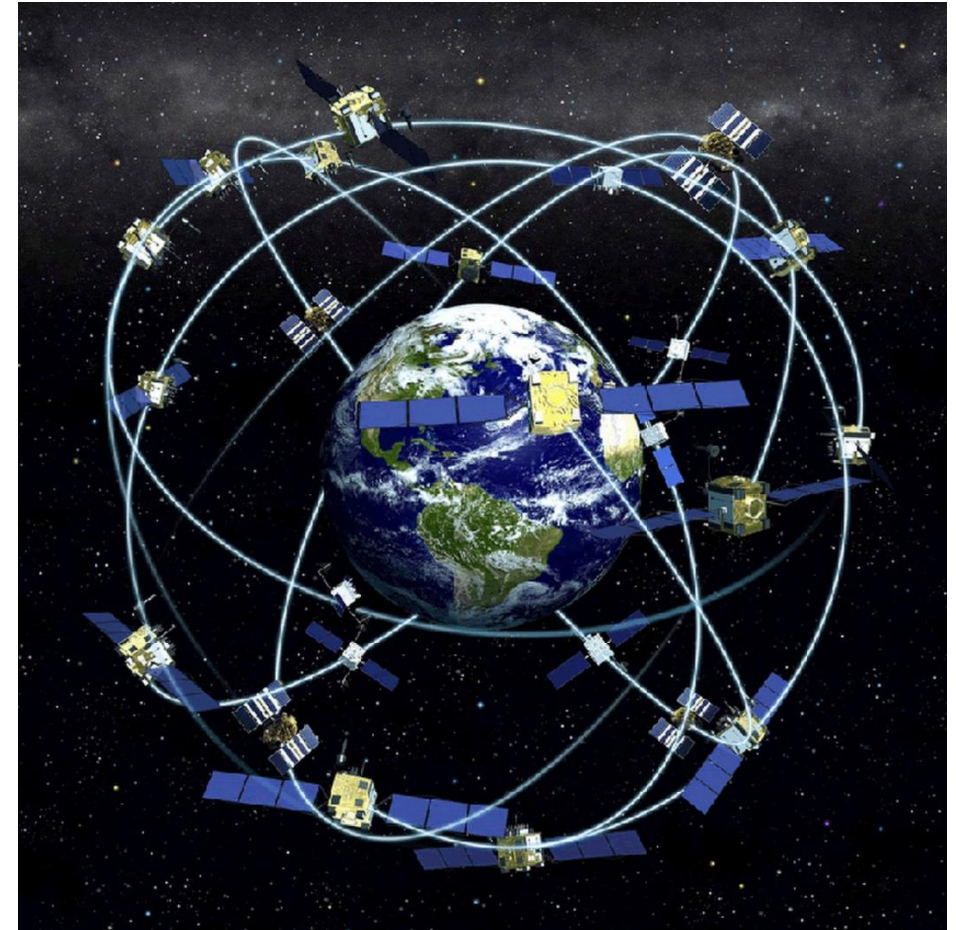
Broadcast two frequencies in L1 and
L2 bands (1.57 and 1.23 GHz).

Other similar GNSS systems:

GLONASS, Galileo, Beidou

Ionosphere is a dispersive media

Total electron content (TEC) along the signal path
from GPS spacecraft to the receiver can be inferred
by measuring the phase advance and/or the group
delay between different frequencies.



GNSS tomography example-1

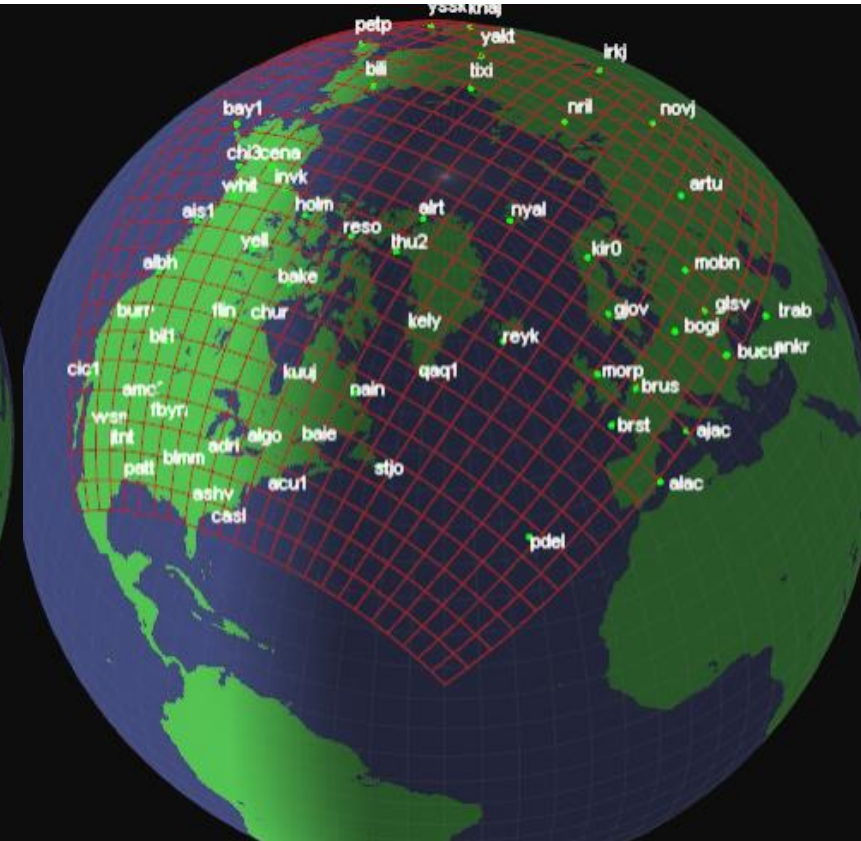
Network of ground dual-frequency GNSS receivers at high latitudes.

Tomographic inversion of the GNSS data should reveal plasma dynamics.

Network of GNSS receivers



Projection of the tomographic grid

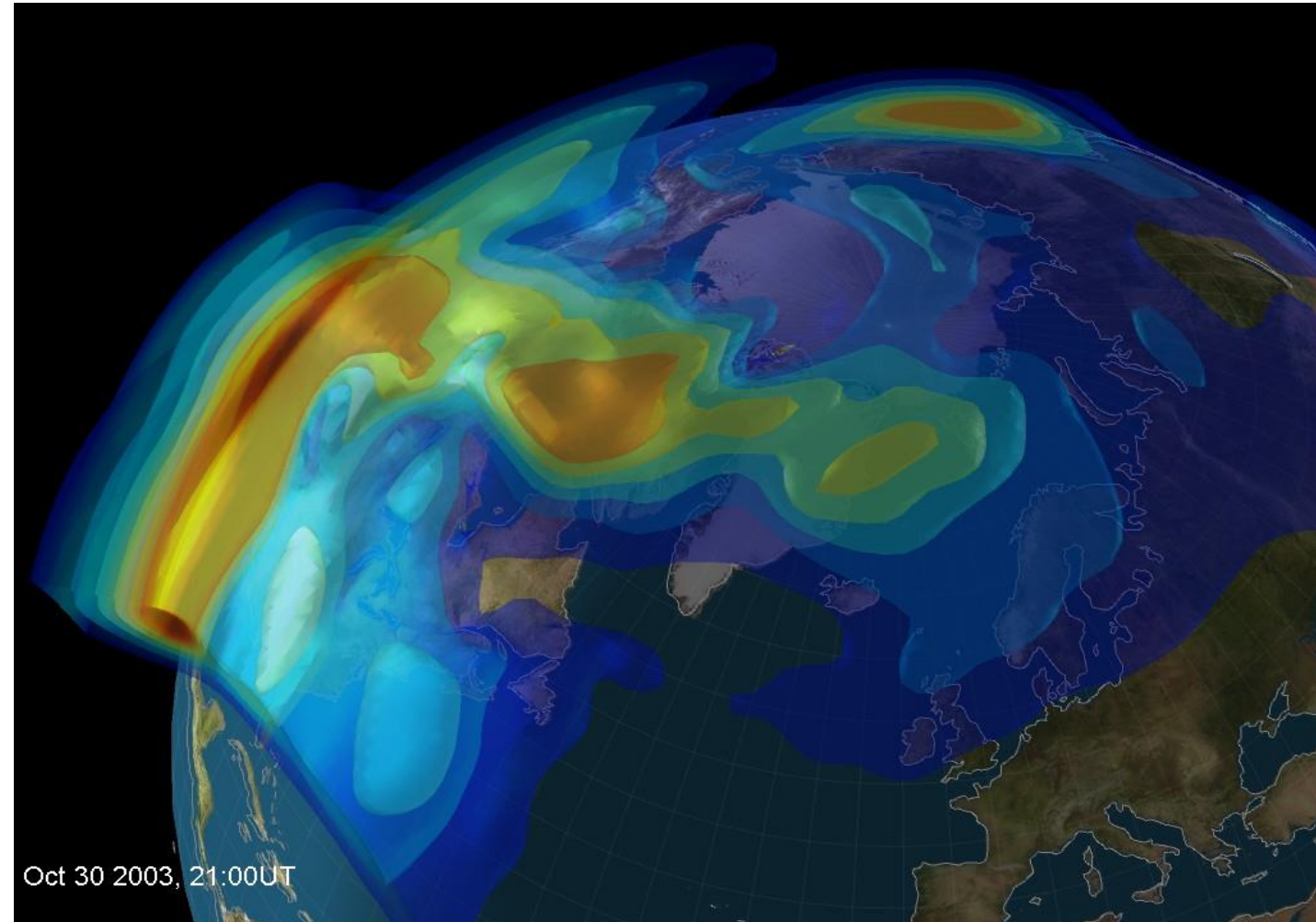


GNSS tomography example-3

Results of the tomographic reconstruction: plasma density

The global distribution of ionospheric plasma density can be deduced from characteristics of GPS signals acquired by ground-based network of GPS receivers.

Plasma follows general anti-sunward cross-polar convection.

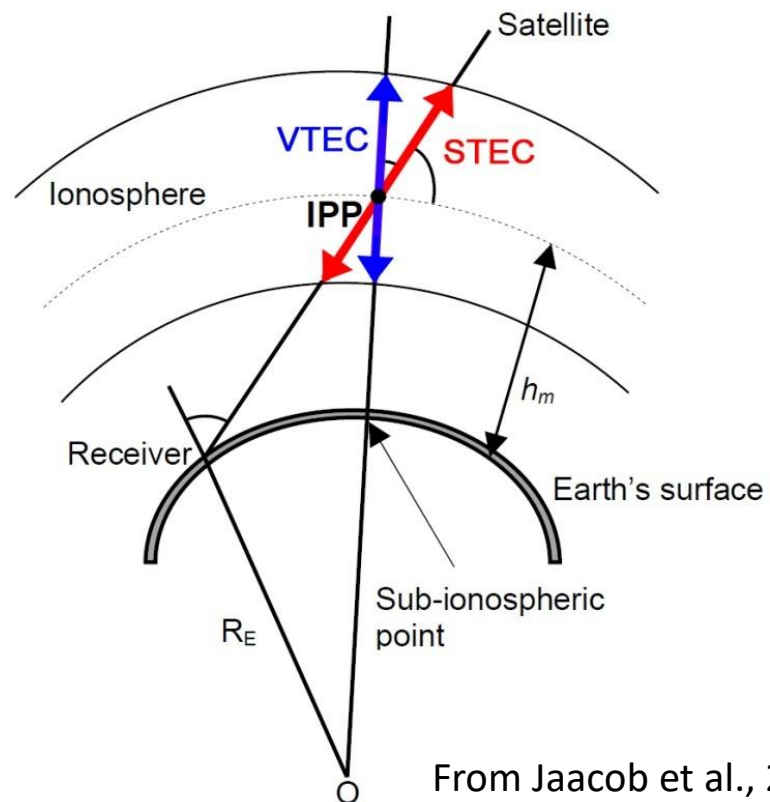


Mitchell et al, AGU Monograph 2008, doi:10.1029/181GM09

Direct reconstruction of VTEC

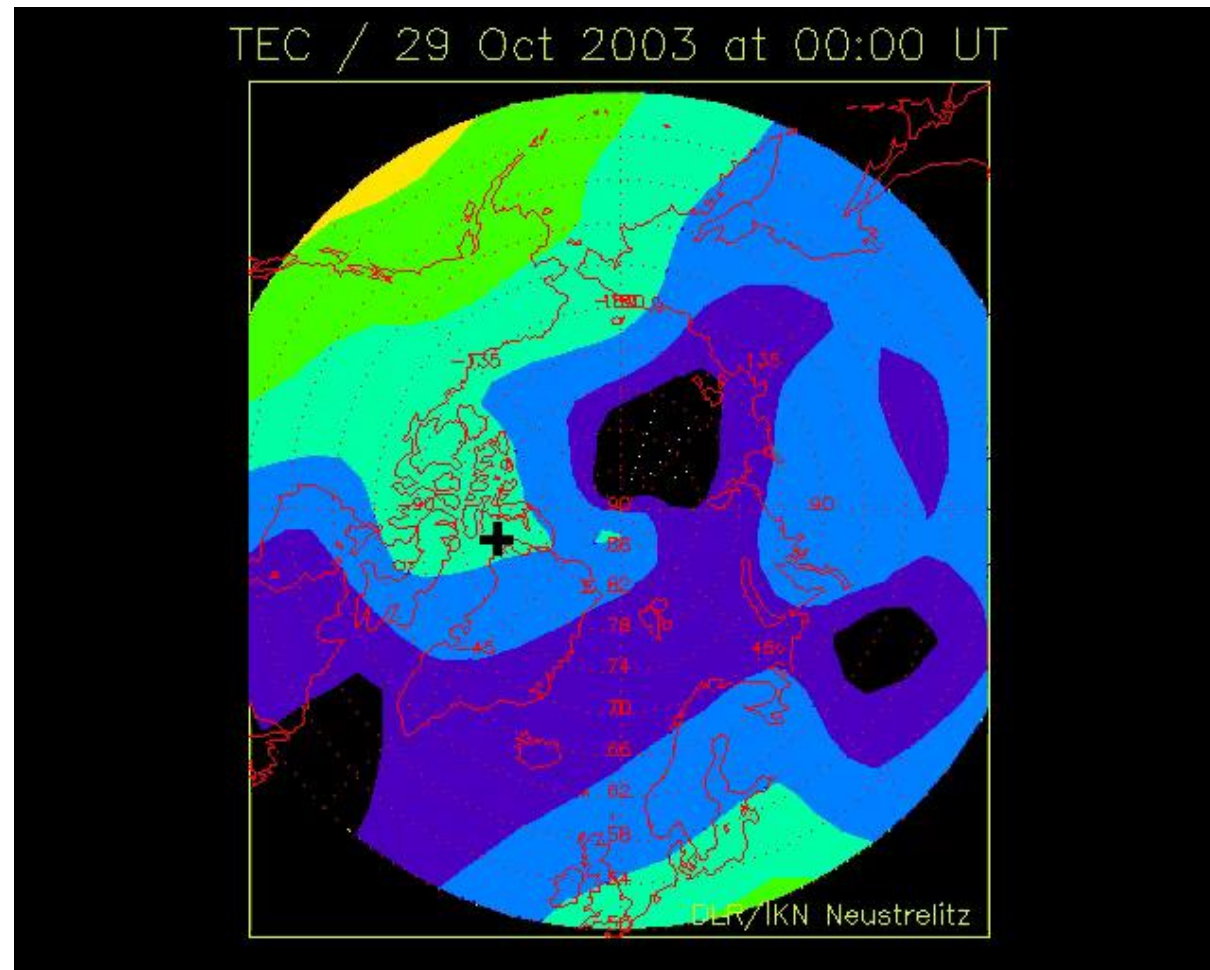
Simpler direct reconstructions are also possible.

Only assumptions about ionospheric equivalent height are needed.



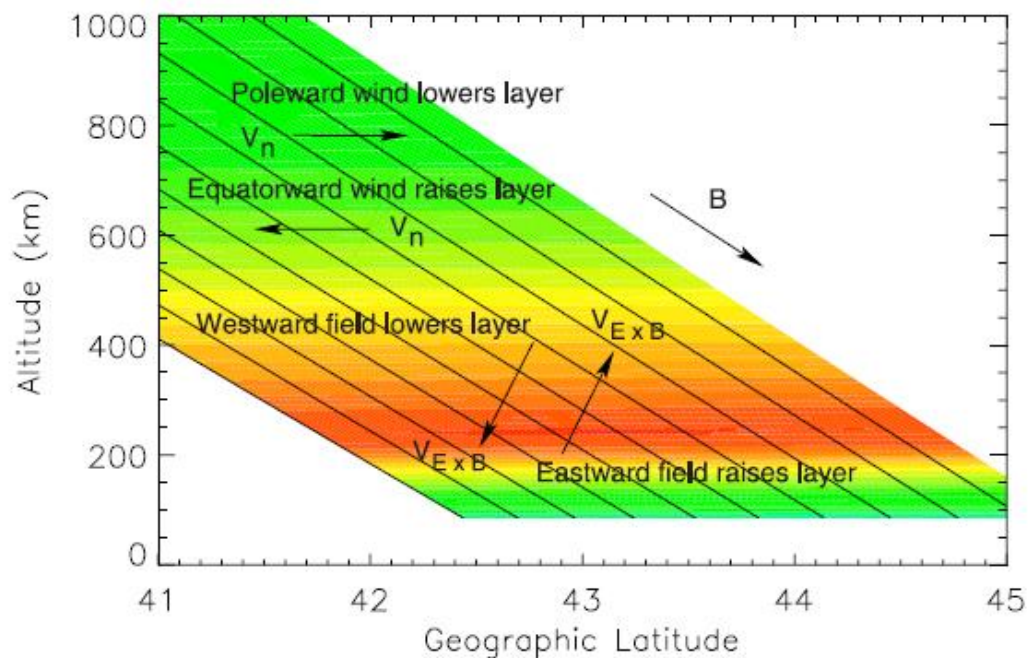
From Jacob et al., 2008

Jakowski et al., JASTP, 2005, doi:10.1016/j.jastp.2005.02.023

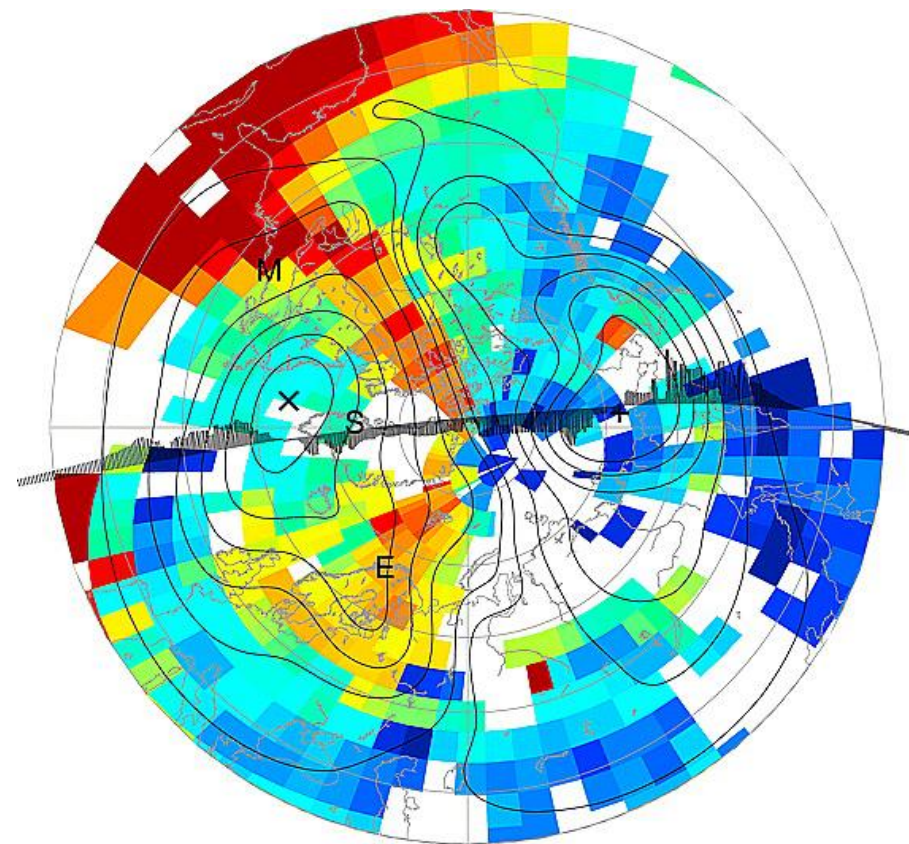


Formation of polar tongue of ionisation during storms

- Neutral winds can push plasma along (up) the field lines, to where the plasma recombination rate is slower.
- $E \times B$ drift may have a vertical component at mid-latitudes.
- Other mechanisms (e.g., chemical or compositional changes) could be more important during storm recovery phases.



Swisdak et al., 2006, doi:10.1029/2005GL024973

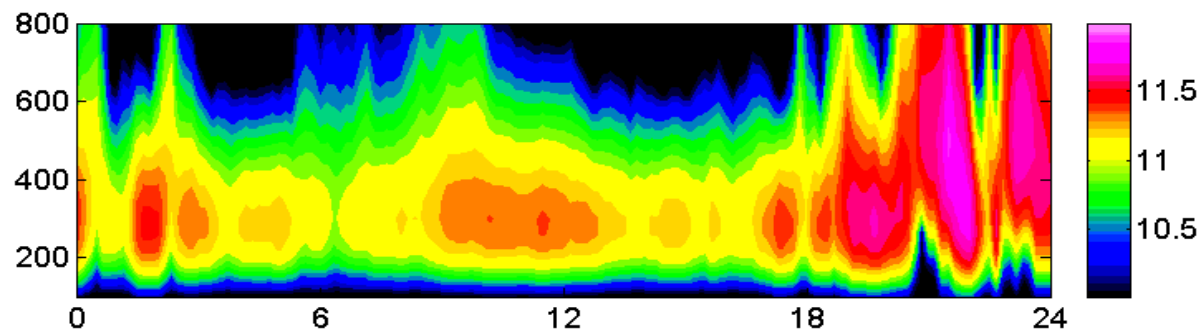


Foster et al., 2005, doi:10.1029/2004JA010928

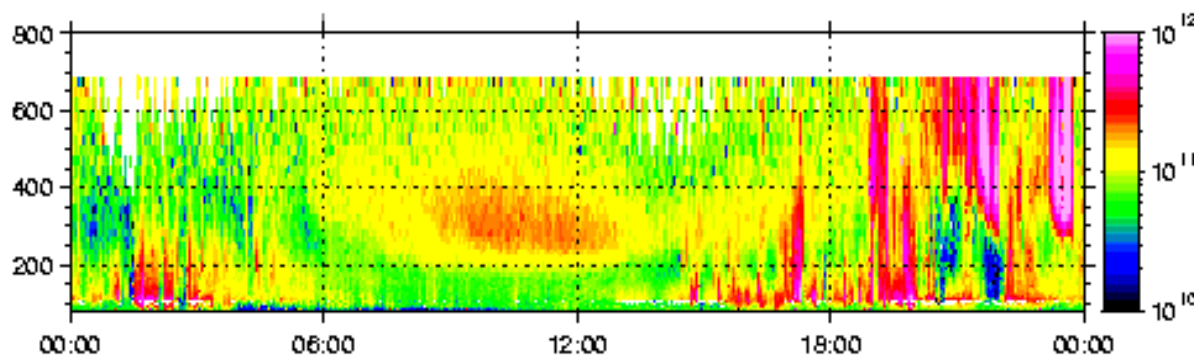


Comparison with radar observations

Electron density during 30-Oct-2003 storm as a function of height and UT



Tomography
propagated across
the polar cap



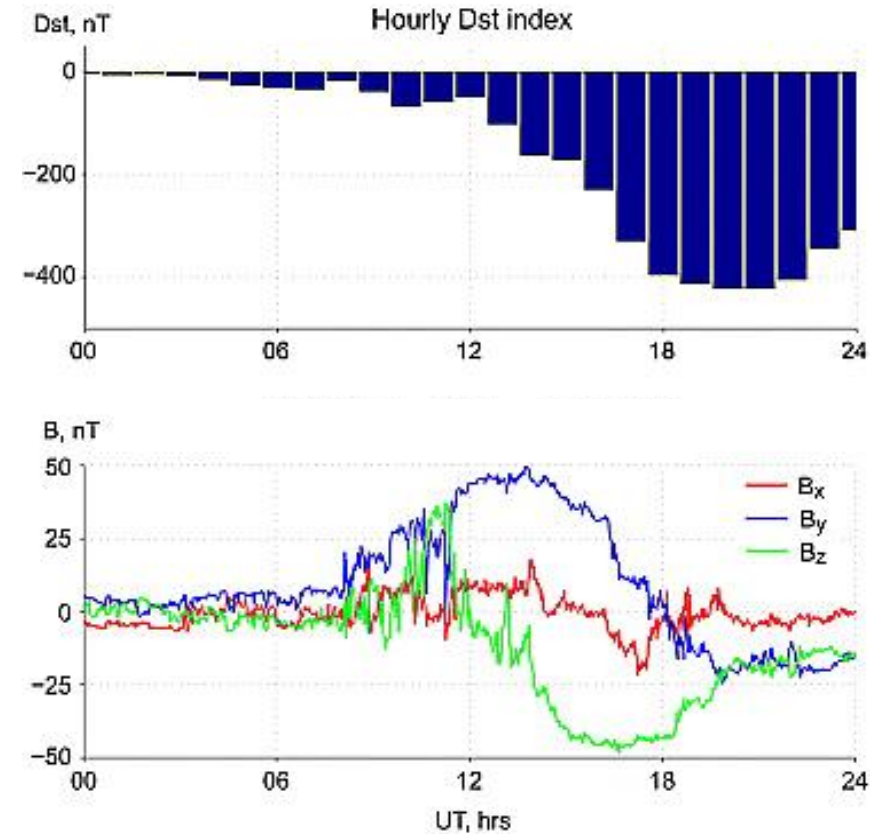
EISCAT radar in
Scandinavia

Mitchell and Spencer, 2007, doi:10.4401/ag-3074



Example: 20-Nov-2003 geomagnetic superstorm

- The storm is isolated with a quiet pre-storm day (19-Nov).
- Formation of the high-latitude anomaly is expected during the main phase (12 - 21UT).
- The tongue would be forming in North American sector (dayside during the main phase) spreading anti-sunward.
- More on the 20-Nov-2003 superstorm:
 - Foster et al., 2005, doi:10.1029/2004JA010928
 - Pokhotelov et al., 2008, doi:10.1029/2008JA013109
 - Pokhotelov et al., 2021, doi:10.5194/angeo-39-833-2021

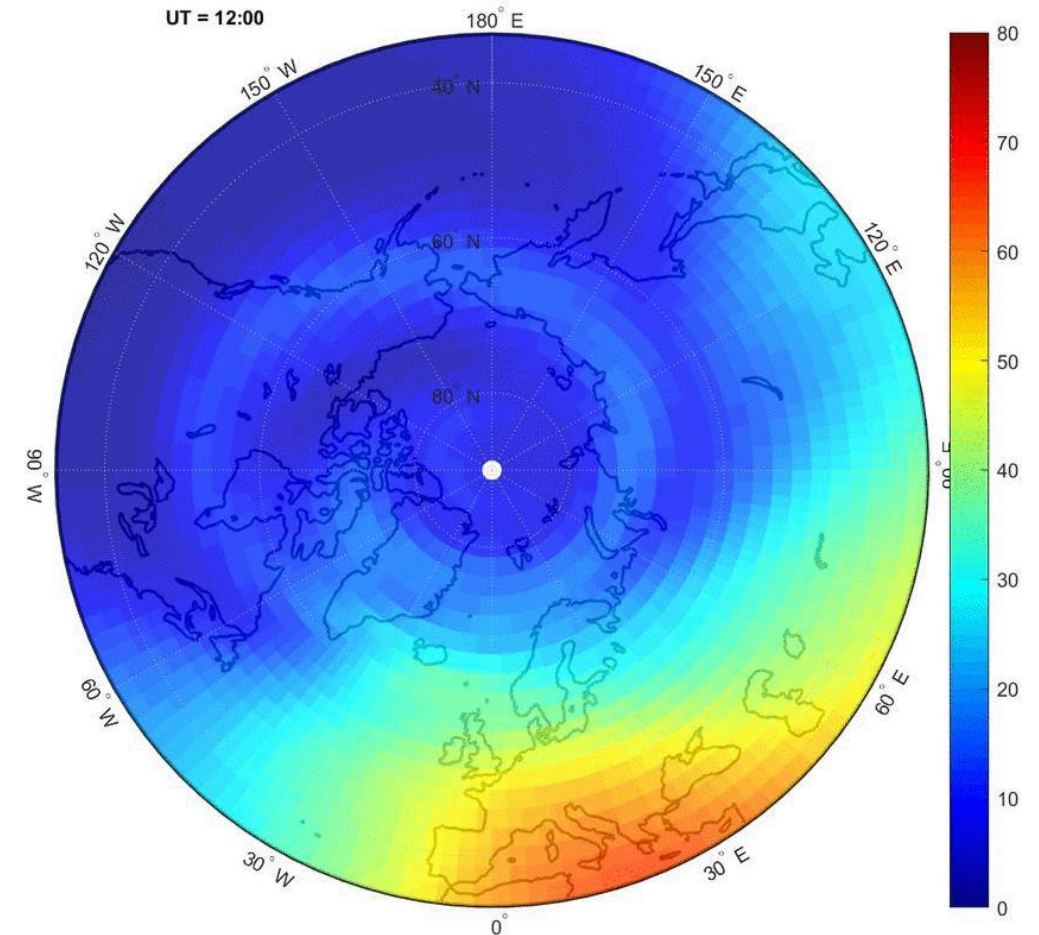


Pokhotelov et al., 2008
doi:10.1029/2008JA013109



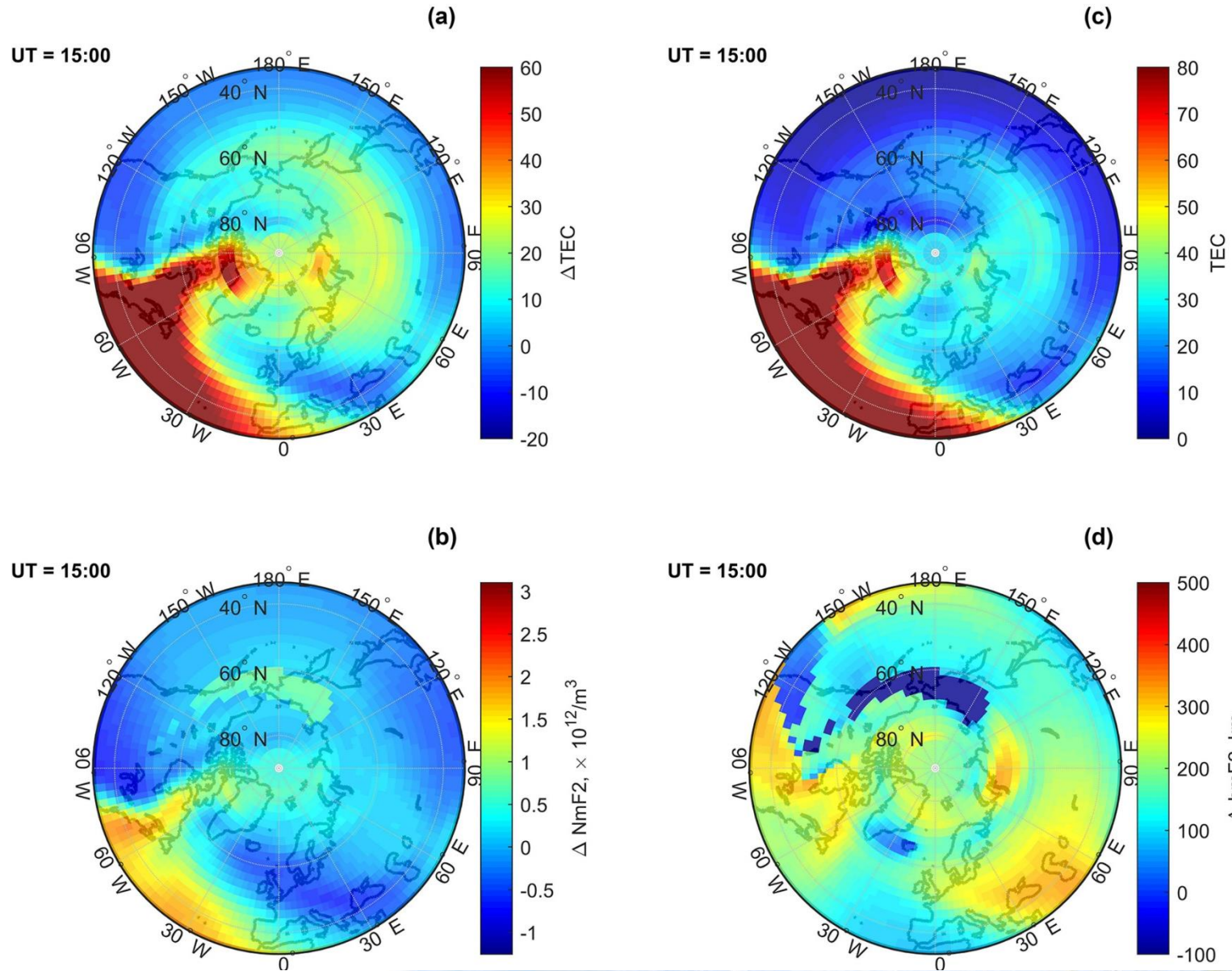
TIE-GCM Simulations: polar cap view

- TIE-GCM simulation of the TOI with Weimer model.
- Animated polar projections (above 30°N).
- TOI maximises over North American Atlantic sector during the main phase (16-18 UT).
- At 18-20 UT large amounts of transported plasma reach over the polar cap into Scandinavian sector.



Pokhotelov et al., 2021, doi:10.5194/angeo-39-833-2021

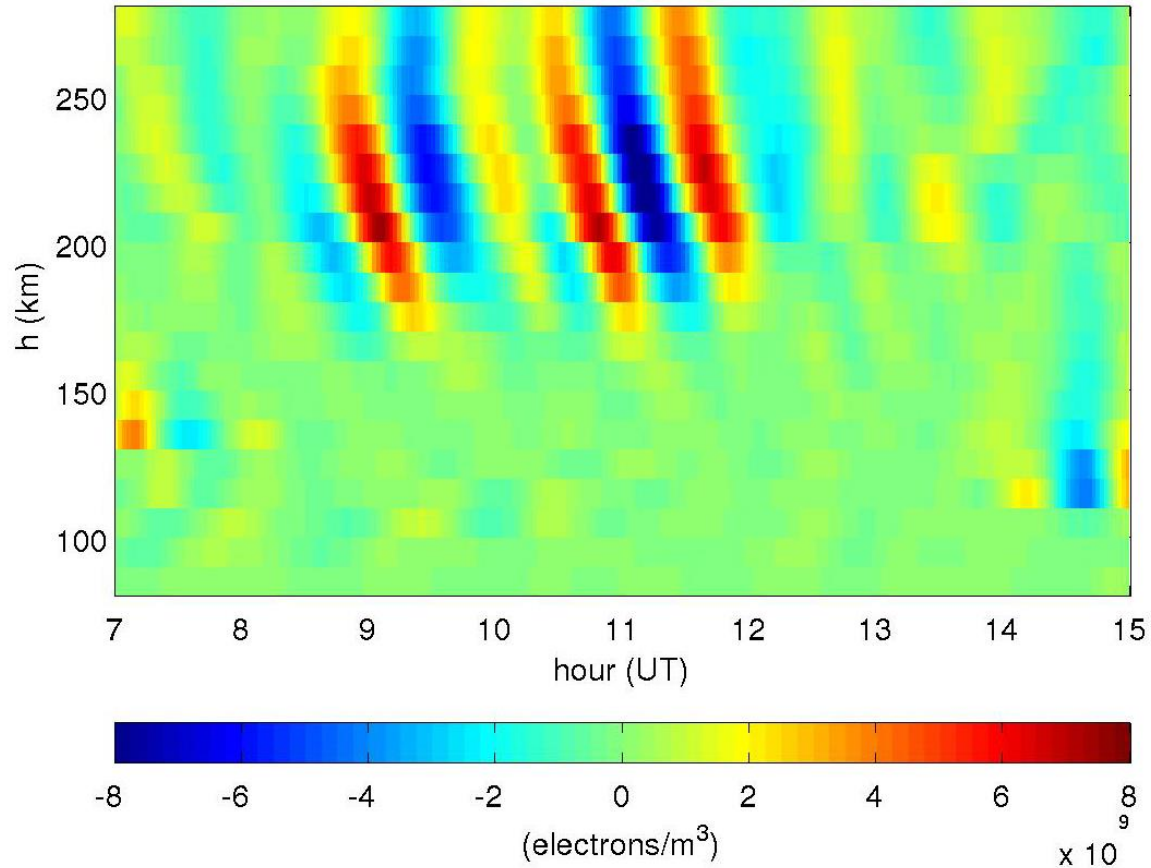
TEC and simulated ionospheric heights from TIEGCM



Pokhotelov et al., 2021
doi:10.5194/angeo-39-833-2021

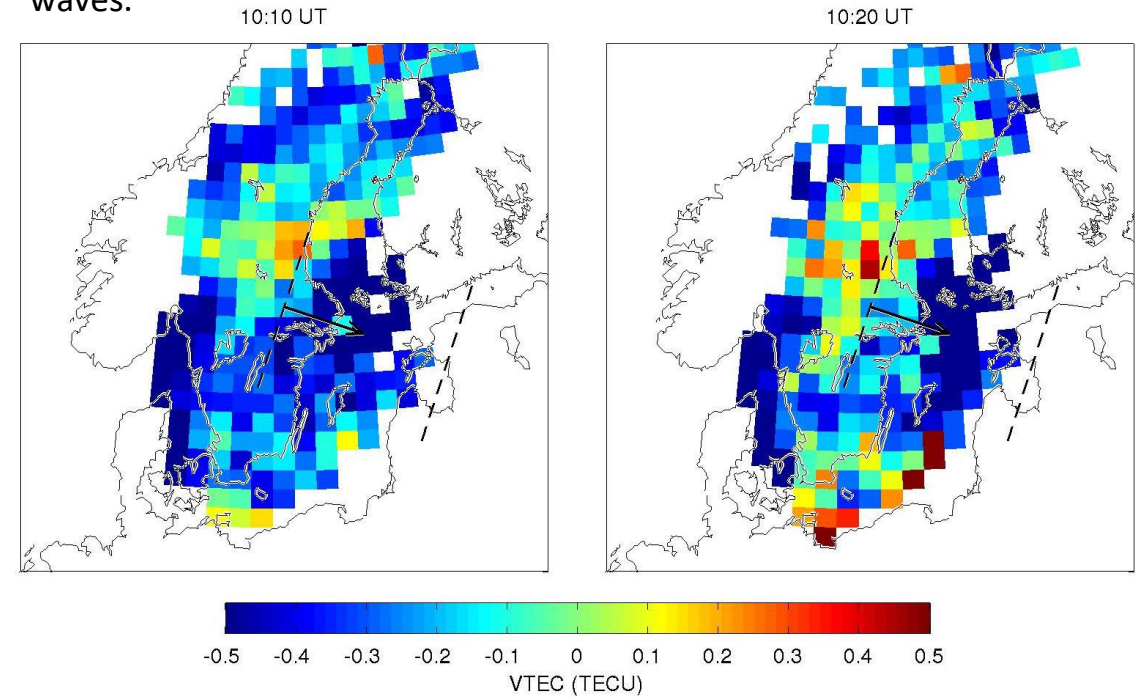
Ionospheric waves in GNSS and ISR data

20 January 2010; Tromsø; electron density filtered at period 1.05 h



Travelling ionospheric disturbances (TIDs) can be sensed simultaneously by EISCAT radar (vertical structure) and by GNSS receiver network (horizontal structure).

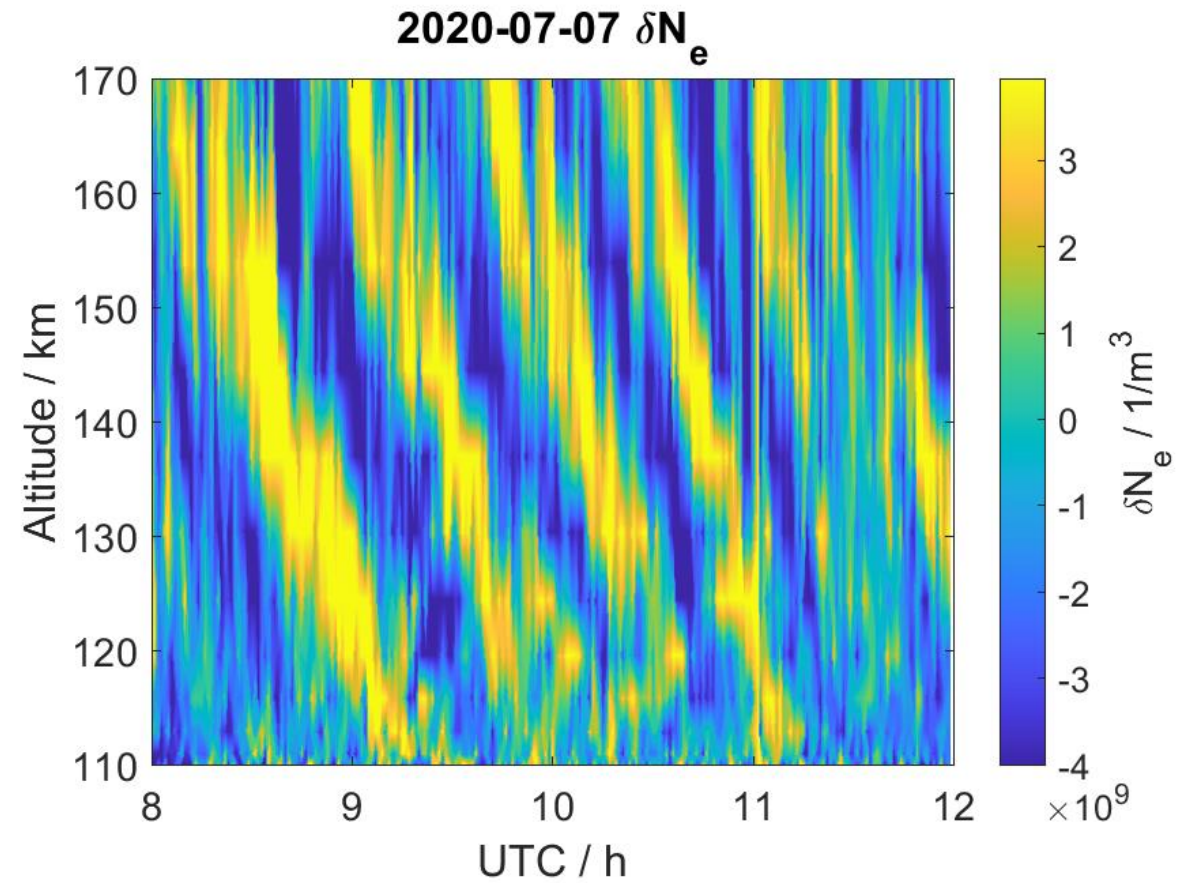
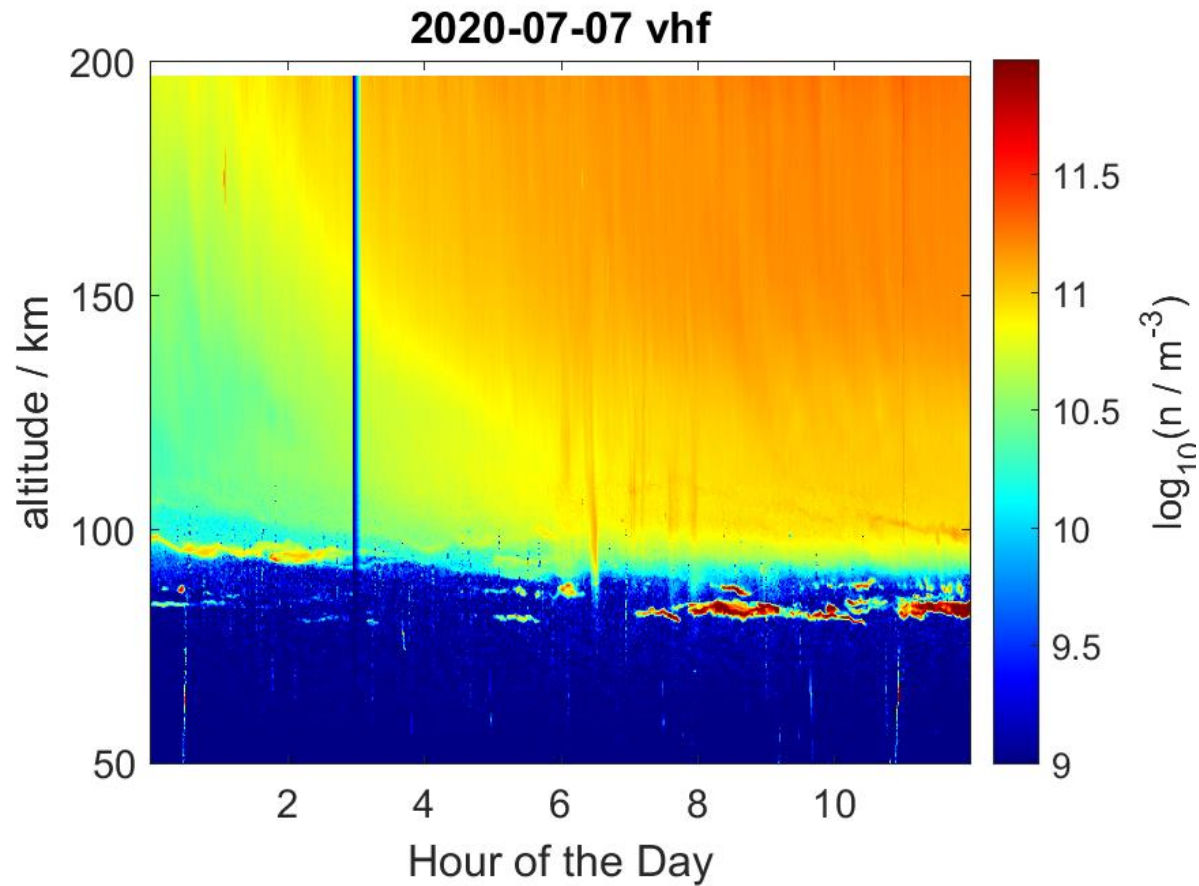
The analysis of GNSS data (~ 200 receivers in Sweden) was inspired by Japanese research (e.g., Tsugawa et al. 2004) on detecting ionospheric effects from extra-long “pre-tsunami” waves.



van der Kamp et al, 2014 doi:10.5194/angeo-32-1511-2014



Neutral winds and TIDs from EISCAT



Bistatic EISCAT experiment from 2020
(jointly with Univ. of Bern and Univ. of Tromsøe)

Günzkofer et al., in preparation



Frictional heating theory, models and measurements

$$T_i = T_n + \frac{m_n}{3k} (u_i - u_n)^2 = T_n + \frac{25}{3} \cdot 10^{-4} \cdot (u_i - u_n)^2$$

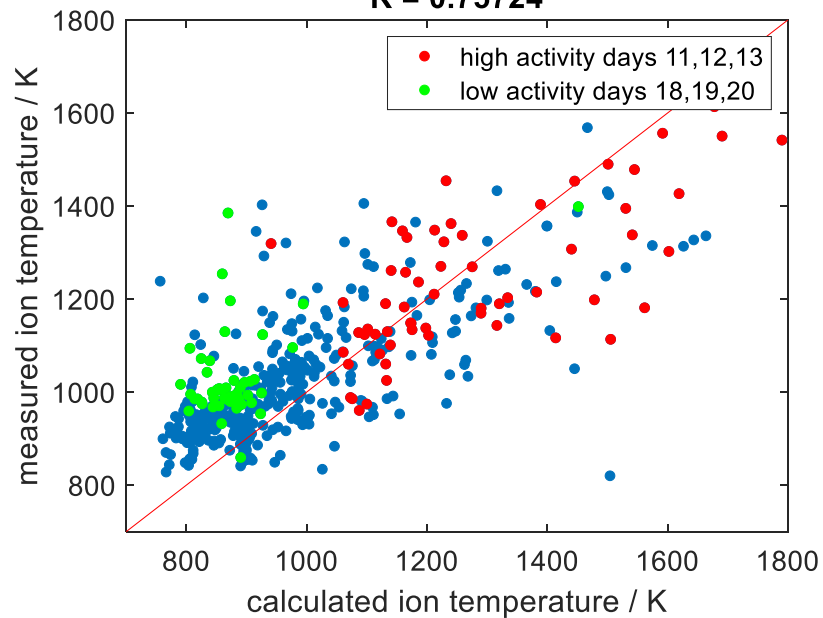
$$\frac{m_n}{3kB^2} = 0.33 \cdot 10^6$$

$T_n; u_n$: model neutral atmosphere

at 300 km

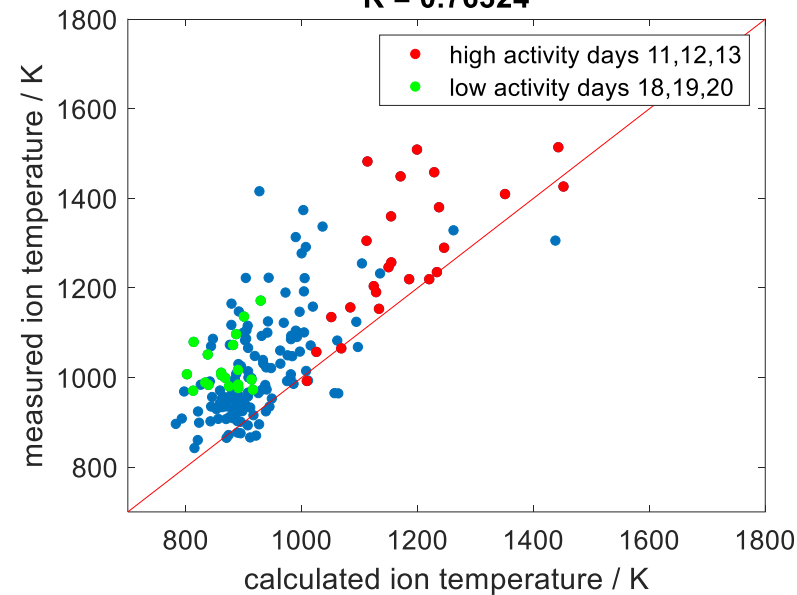
u_i : EISCAT

$R = 0.75724$



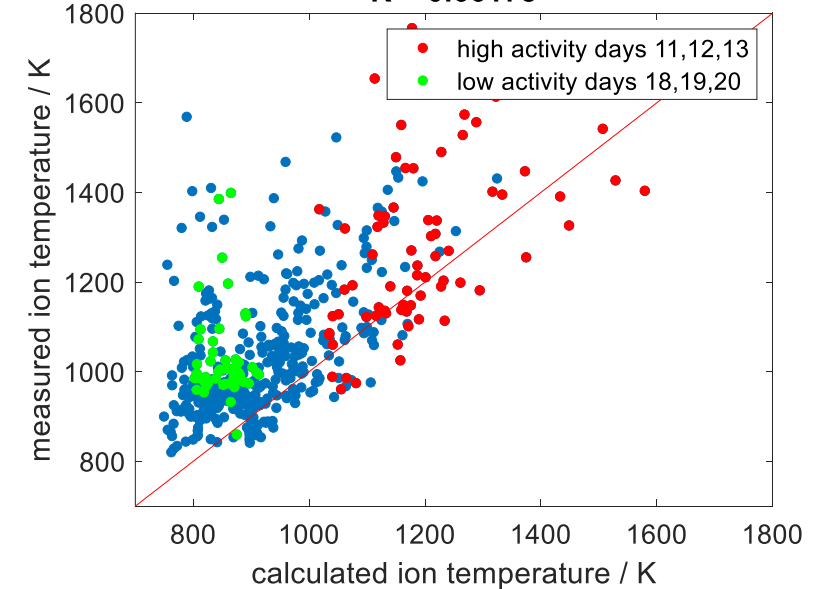
u_i : WACCM-X SD

$R = 0.76324$



u_i : TIE-GCM

$R = 0.66178$



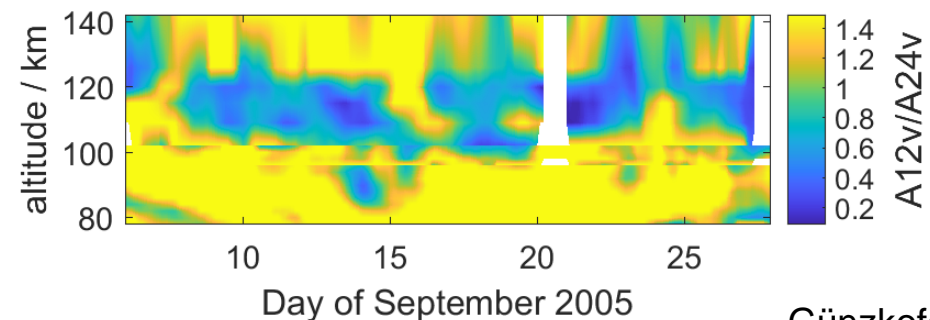
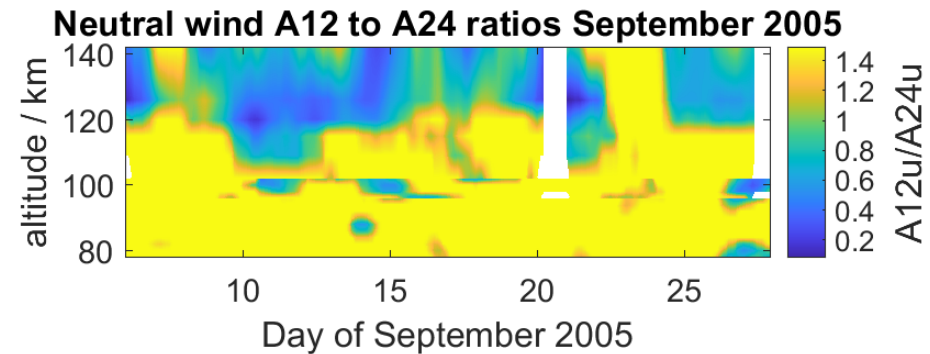
Günzkofer et al., in preparation



Dominant semidiurnal tide above 120 km

Plot semidiurnal (A12) to diurnal (A24) amplitude ratio to find dominant forcing:

- **zonal component:**
expected transition from semidiurnal to diurnal modulations at ~120 km
- **meridional component:**
two-band structure with **unexpected** semidiurnal modulations above ~130 km (mostly before September 17).

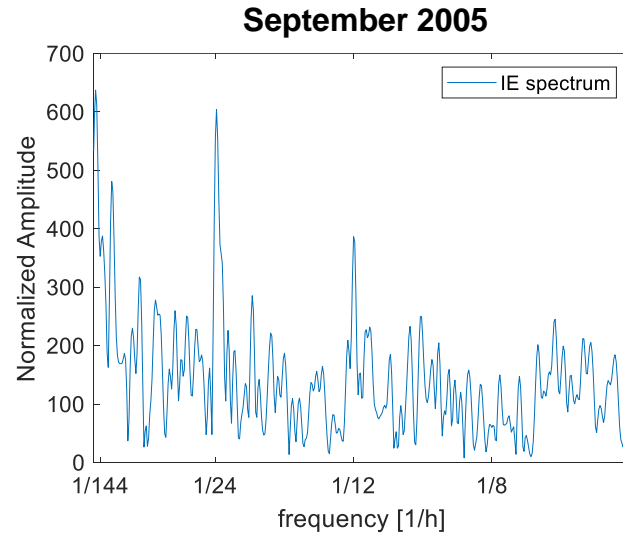


Günzkofer et al., 2022, doi:10.1029/2022JA030861



Geomagnetic impact of tides in AE and IE indices

- Auroral Electrojet (AE) index uses stations along auroral zone → global
- Image Electrojet (IE) index → allows local selection of stations in Fennoscandia



- 'Lat 66-71' subset shows both 24h and 12h modulations

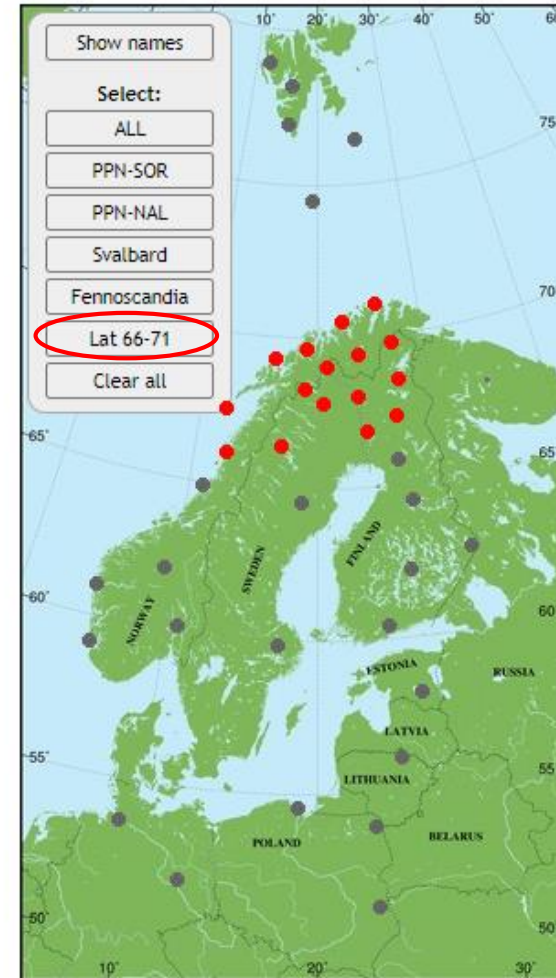


[IMAGE magnetometer network
https://space.fmi.fi/image/www/station_selection.html]

Summary: neutral dynamics issues

- There seem to be a mismatch between polar cap neutral winds, produced by different circulation models (WACCM-X, GAIA, etc.).
- Number of earlier works (e.g., Burns et al., 2004; Liu et al., 2016) suggested that neutral winds during geomagnetic storms blow generally anti-sunward across the polar cap, following much faster plasma drifts.
- The anti-sunward neutral wind can be due to enhanced ion drag imposed by the ion drifts.
- An efficiency of such drag mechanism needs to be validated, especially at lower altitudes of the transition region (~120km).



Summary: plasma dynamics issues

- There is a mismatch between polar cap ExB plasma convection, produced by different convection models (Heelis, Weimer, SuperDARN, AMIE, etc.), especially in the extent of how far the ExB convection expands during geomagnetic storms.
- Electrodynamical transport plays the dominant role in the storm main phase, in the recovery phase a complex interplay between different mechanisms is involved.
- Relative roles of co-rotational and convective forces are poorly understood.
- Mechanisms of plasma uplifts at middle (sub-auroral) latitudes need to be understood, but difficult to measure. Mid-latitude SuperDARN and/or incoherent scatter radars should be used.



Summary of recent results, relevant to the IMAGE network

- EISCAT radar data show a complex mixture of semi-diurnal and diurnal tidal oscillations in high-latitude ionosphere. Three ionospheric models (GAIA, SD-WACCM-X, TIE-GCM) support the observed tidal structure and allow to determine the forcing from above and below.
- The impact of both diurnal and semidiurnal variations is seen in the IMAGE magnetometer data, due to a tidal impact on the ionospheric transition region.
- Further joint studies needed with the EISCAT and Fennoscandian instrument networks.



References (underlined are the contributors of this presentation)

- Jakowski et al, JASTP, 2005 <https://doi.org/10.1016/j.jastp.2005.02.023>
- Mitchell, Yin, Spencer, Pokhotelov, AGU Monograph 181, 2008, <https://doi.org/10.1029/181GM09>
- Pokhotelov, Mitchell, Spencer, Hairston, Heelis, JGR, 2008 <https://doi.org/10.1029/2008JA013109>
- van der Kamp, Pokhotelov, Kauristie, AG, 2014 <https://doi.org/10.5194/angeo-32-1511-2014>
- Pokhotelov, Fernandez-Gomez, Borries, AG, 2021 <https://doi.org/10.5194/angeo-39-833-2021>
- Günzkofer, Pokhotelov, et al., JGR, 2022 <https://doi.org/10.1029/2022JA030861>



Further info, and the current presentation for download:

<https://www.researchgate.net/profile/Dimitry-Pokhotelov>

